



Original article

Novel β -carboline-tripeptide conjugates attenuate mesenteric ischemia/reperfusion injury in the ratWei Bi^{c,*}, Yue Bi^d, Ping Xue^c, Yanrong Zhang^c, Xiang Gao^c, Zhibo Wang^c, Meng Li^c, Michele Baudy-Floc'h^e, Nathaniel Ngerebara^a, Xiaoxu Li^f, K. Michael Gibson^b, Lanrong Bi^{a,**}^a Department of Chemistry, Michigan Technological University, Houghton, MI 49931, USA^b Department of Biological Sciences, Michigan Technological University, Houghton, MI 49931, USA^c Department of Surgery, Second Hospital of HeBei Medical University, Shijiazhuang 050000, PR China^d School of Basic Medical Sciences, HeBei Medical University, Shijiazhuang 050000, PR China^e UMR 6226 CNRS, ICMV, Sciences Chimiques de Rennes, Université de Rennes 1, F-35042 Rennes Cedex, France^f Columbia University College of Physicians and Surgeons, Columbia University, New York, NY 10027, USA

ARTICLE INFO

Article history:

Received 6 January 2011

Received in revised form

28 February 2011

Accepted 14 March 2011

Available online 21 March 2011

Keywords:

Ischemia/reperfusion injury

Anti-inflammatory activity

Analgesic activity

 β -carboline-tripeptide conjugate

ABSTRACT

We have synthesized a series of new β -carboline-tripeptide conjugates, and examined their anti-inflammatory properties in a mouse model of xylene-induced ear edema. The analgesic capacity of these compounds was further evaluated in a rodent tail flick assay. Our results indicate that β -carboline conjugate **4a** manifests potent anti-inflammatory and analgesic activity while exerting a protective effect against mesenteric ischemia/reperfusion (I/R) injury in the rat.

Published by Elsevier Masson SAS.

1. Introduction

Mesenteric ischemia is frequently encountered in multiple disease states and surgical procedures, including cardiovascular interventions, small bowel transplantation mesenteric thrombosis, shock syndromes, and severe burns [1,2]. The ensuing reperfusion is unavoidable and may induce downstream tissue injury. Intestinal ischemia and reperfusion injury can accelerate interactions between endothelium and different cell types resulting in microvascular injury, cellular necrosis, and apoptosis [3–7]. During intestinal ischemia/reperfusion, reactive oxygen species (ROS) attack constituents of the cell membrane constituents, resulting in lipid peroxidation, membrane disintegration, and increased microvascular permeability. The latter induces activation and adhesion of polymorphonuclear neutrophils (PMNs), the release of proinflammatory substances, and increased formation of ROS. The intestine is highly sensitive to ischemic injury. Activated

neutrophils in this tissue enhance ROS and cytotoxic protein production, leading to an induction of the inflammatory cascade [3,4], resulting in cell death and organ failure. To counter these processes, various therapeutic strategies have been attempted to attenuate intestinal ischemia/reperfusion injury, including anti-leukocyte and anti-inflammatory therapies, as well as glutamine, glycine and antioxidant supplementation [5,8].

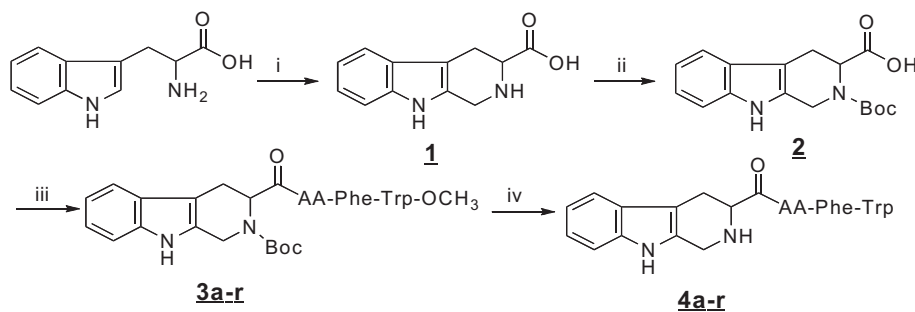
β -Carbolines possess potential antioxidant properties. For example, harmaline, harmaline and harmalol inhibit lipid peroxidation in microsomal hepatic preparations [9] and through attenuation of oxidative damage of hyaluronic acid, cartilage collagen and immunoglobulin G [10]. Other findings suggest that β -carboline alkaloids exert a protective effect via ROS scavenging [11–13].

It has been reported that some short peptides with certain sequences may be used as analgesic agents [14]. In addition, our recent research findings indicated that some tripeptides with AA-Phe-Trp sequence present good analgesic activities. Since reactive oxygen species (ROS) and inflammatory leukocytes play an important role in the pathogenesis of I/R injury, antioxidant therapy and inhibition of post-ischemic neutrophil infiltration may have therapeutic efficacy during I/R injury. Ideally, I/R injury can be

* Corresponding author. Tel./fax: +86 311 66002578.

** Corresponding author. Tel.: +1 906 487 1868; fax: +1 906 487 2061.

E-mail addresses: biwei8115@sohu.com (W. Bi), lanrong@mtu.edu (L. Bi).



Scheme 1. Synthetic scheme for β -carboline-tripeptide conjugates preparation. Reagents and conditions: (i) formaldehyde and sulfuric acid; (ii) Boc-N₃ and triethylamine; (iii) HCl·L-AA-Phe-Trp-OCH₃ and DCC; (iv) HF.

treated by a combination of the therapeutic agents. Generally, when two synergistic agents are administered individually but simultaneously, they will be transported to the site of action with different efficiencies. However, there are potential advantages in giving the co-administered agents as a single chemical entity. It is desirable to have the two synergistic agents reach a site simultaneously. Considering the antioxidant properties of β -carboline

alkaloids coupled with the analgesic activity observed with AA-Phe-Trp tripeptides, we hypothesized that β -carboline and tripeptide (AA-Phe-Trp) conjugates might exhibit both enhanced antioxidant and analgesic activities. To test this hypothesis, we have synthesized a series of novel β -carboline-tripeptide (AA-Phe-Trp) conjugates, and evaluated their biological capacity to protect against mesenteric I/R injury.

Table 1
In vivo orally analgesic activities of **4a–r** tested using tail flick method in mice.

Compd.	Pain threshold variation ($X \pm SD\%$)					
	30 min	60 min	90 min	120 min	150 min	180 min
NS	5.03 \pm 10.26	7.45 \pm 8.03	7.53 \pm 11.54	8.09 \pm 13.28	9.02 \pm 12.19	8.75 \pm 9.73
Morphine	142.20 \pm 35.43	175.78 \pm 63.21	139.03 \pm 49.35	98.78 \pm 38.43	64.55 \pm 25.61	57.43 \pm 31.08
Aspirin	32.85 \pm 10.46 ^a	38.45 \pm 12.13 ^a	41.23 \pm 15.76 ^a	33.24 \pm 18.32 ^a	30.41 \pm 8.98 ^a	21.72 \pm 9.74 ^b
4a	48.25 \pm 45.02 ^a	59.37 \pm 37.02 ^a	44.67 \pm 41.08 ^a	34.55 \pm 38.43 ^a	25.46 \pm 12.12 ^b	18.86 \pm 19.46
4b	10.36 \pm 22.24	40.78 \pm 32.03 ^b	46.45 \pm 5.46 ^b	49.09 \pm 29.03 ^a	22.37 \pm 34.30 ^b	14.36 \pm 28.12
4c	23.17 \pm 25.32	49.74 \pm 35.11 ^a	21.35 \pm 27.20	18.79 \pm 15.74	25.05 \pm 18.13 ^b	15.68 \pm 11.32
4d	39.47 \pm 25.44 ^a	45.77 \pm 26.32 ^a	47.36 \pm 28.21 ^a	35.79 \pm 9.32 ^b	25.88 \pm 11.77 ^b	16.03 \pm 8.96
4e	37.58 \pm 20.23 ^a	48.23 \pm 14.23 ^a	46.48 \pm 9.15 ^a	42.03 \pm 6.41 ^a	28.79 \pm 10.13 ^b	19.22 \pm 17.46
4f	31.34 \pm 31.32 ^a	37.20 \pm 15.13 ^b	40.56 \pm 8.32 ^b	45.46 \pm 23.54 ^b	21.12 \pm 14.45 ^b	15.32 \pm 11.18
4g	33.01 \pm 38.16 ^a	38.01 \pm 29.23 ^a	41.23 \pm 44.46 ^a	27.32 \pm 14.88 ^b	15.25 \pm 22.46	16.13 \pm 13.39
4h	35.05 \pm 29.27 ^a	36.45 \pm 27.36 ^a	35.19 \pm 21.33 ^a	28.55 \pm 12.36	16.69 \pm 10.33	14.23 \pm 12.18
4i	30.75 \pm 24.24 ^a	38.20 \pm 32.09 ^a	40.36 \pm 23.49 ^a	42.43 \pm 27.22 ^b	23.19 \pm 15.36 ^b	19.25 \pm 14.39
4j	37.25 \pm 21.12 ^a	32.19 \pm 14.78 ^b	22.23 \pm 14.66	39.38 \pm 13.48 ^b	24.33 \pm 6.49 ^b	13.29 \pm 12.47
4k	44.27 \pm 42.46 ^a	52.22 \pm 33.12 ^a	54.39 \pm 23.67 ^a	41.28 \pm 13.33 ^a	29.04 \pm 22.58 ^b	25.69 \pm 11.36 ^b
4l	41.83 \pm 39.35 ^a	47.33 \pm 19.47 ^b	51.25 \pm 11.84 ^a	32.33 \pm 22.89	18.32 \pm 37.12	22.45 \pm 43.22 ^b
4m	21.24 \pm 15.74 ^b	45.23 \pm 11.14 ^a	34.56 \pm 35.77 ^b	39.25 \pm 17.48 ^b	22.12 \pm 26.22 ^b	19.45 \pm 21.79
4n	30.56 \pm 21.46 ^a	42.32 \pm 16.41 ^b	44.13 \pm 28.22 ^a	38.45 \pm 19.66 ^b	26.47 \pm 27.55 ^b	25.07 \pm 11.21 ^b
4o	35.75 \pm 30.35 ^a	41.18 \pm 17.45 ^a	43.23 \pm 32.49 ^a	30.25 \pm 31.49 ^b	28.87 \pm 21.93 ^b	20.94 \pm 14.46 ^b
4p	38.16 \pm 19.26 ^a	35.13 \pm 22.25 ^a	46.08 \pm 19.94 ^a	37.12 \pm 15.25 ^b	29.38 \pm 16.45 ^b	21.55 \pm 17.29 ^b
4q	22.17 \pm 28.57 ^b	28.12 \pm 19.81 ^b	34.55 \pm 13.29 ^b	40.67 \pm 33.57 ^a	13.54 \pm 18.46	18.77 \pm 13.45
4r	18.24 \pm 11.56	17.23 \pm 13.55	29.25 \pm 17.12 ^b	39.23 \pm 27.12 ^b	12.25 \pm 26.18	12.32 \pm 14.94

NS = vehicle; $n = 10$; oral dose of **4a–r** = 0.15 mmol/kg; intraperitoneal dose of morphine = 0.15 mmol/kg. Oral dose of aspirin = 0.15 mmol/kg.

^a Compared with vehicle $P < 0.01$.

^b Compared with vehicle $P < 0.05$.

Table 2
Analgesic activities of **4a,k** at different doses using tail flick method in mice.

Compd.	Dose	Pain threshold variation ($X \pm SD\%$)					
		30 min	60 min	90 min	120 min	150 min	180 min
NS		5.03 \pm 10.26	7.45 \pm 8.03	7.53 \pm 11.54	8.09 \pm 13.28	9.02 \pm 12.19	8.75 \pm 9.73
4a	0.15 mmol/kg	48.25 \pm 45.02 ^a	59.37 \pm 37.02 ^a	44.67 \pm 41.08 ^a	34.55 \pm 38.43 ^a	25.46 \pm 12.12 ^b	18.86 \pm 19.46
	0.10 mmol/kg	35.41 \pm 13.56 ^a	37.65 \pm 28.53 ^a	32.73 \pm 18.69 ^a	25.45 \pm 15.37 ^b	22.13 \pm 14.89 ^b	13.42 \pm 8.68
	0.05 mmol/kg	29.22 \pm 10.26 ^b	23.45 \pm 15.31 ^b	20.65 \pm 18.94	17.97 \pm 14.64	8.23 \pm 12.04	7.46 \pm 8.95
4k	0.15 mmol/kg	44.27 \pm 42.46 ^a	52.22 \pm 33.12 ^a	54.39 \pm 23.67 ^a	41.28 \pm 13.33 ^a	29.04 \pm 22.58 ^b	25.69 \pm 11.36 ^b
	0.10 mmol/kg	32.32 \pm 19.55 ^b	34.48 \pm 21.03 ^a	38.33 \pm 11.25 ^a	23.08 \pm 13.89 ^b	21.39 \pm 15.60 ^b	14.38 \pm 20.13
	0.05 mmol/kg	11.55 \pm 9.28	26.54 \pm 10.33 ^b	23.58 \pm 11.46 ^b	18.99 \pm 8.96	15.43 \pm 10.94	9.06 \pm 15.43
LFW	0.15 mmol/kg	25.38 \pm 11.85 ^b	28.79 \pm 12.32 ^b	20.13 \pm 8.73	18.92 \pm 9.20	9.77 \pm 2.41	7.98 \pm 2.94
KFW	0.15 mmol/kg	20.16 \pm 9.88 ^b	25.43 \pm 8.79 ^b	23.47 \pm 15.20 ^b	20.14 \pm 11.57	11.23 \pm 7.89	8.41 \pm 5.24

NS = vehicle; $n = 10$.

^a Compared with NS, $P < 0.01$.

^b Compared with NS, $P < 0.05$.

Table 3
Anti-inflammatory activities of **4a–r** against xylene-induced ear edema in mice.

Compd.	Edema weight (X ± SD mg)	Inhibition (%)	Compd.	Edema weight (X ± SD mg)	Inhibition (%)
NS	3.28 ± 0.49		4i	1.62 ± 0.43 ^a	50.6
Aspirin	1.80 ± 0.68 ^a	45.1	4j	1.39 ± 0.28 ^a	57.6
4a	1.29 ± 0.35 ^a	60.7	4k	1.47 ± 0.27 ^a	55.2
4b	2.05 ± 0.76 ^b	37.5	4l	1.89 ± 0.60 ^a	42.4
4c	1.73 ± 0.31 ^a	47.3	4m	1.45 ± 0.42 ^a	55.8
4d	1.85 ± 0.54 ^a	43.6	4n	1.78 ± 0.35 ^a	45.7
4e	1.55 ± 0.43 ^a	52.7	4o	1.61 ± 0.32 ^a	50.9
4f	1.70 ± 0.41 ^a	48.2	4p	1.41 ± 0.49 ^a	57.0
4g	1.43 ± 0.38 ^a	56.4	4q	1.97 ± 0.53 ^b	40.0
4h	1.59 ± 0.44 ^a	51.5	4r	2.35 ± 0.55	28.4

NS = vehicle; n = 10; oral dose of **4a–r** = 0.15 mmol/kg.^a Compared to NS, P < 0.01.^b Compared to NS, P < 0.05.**Table 4**
Anti-inflammatory activities of **4a,c,k,o,p** at different doses.

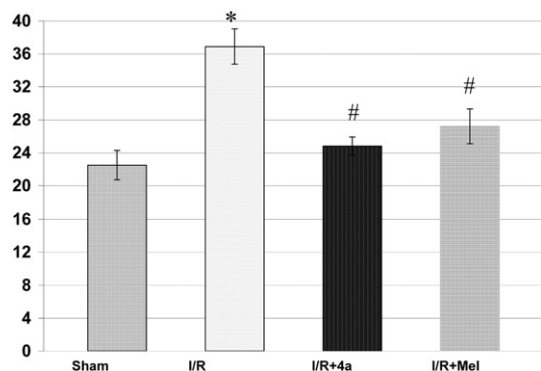
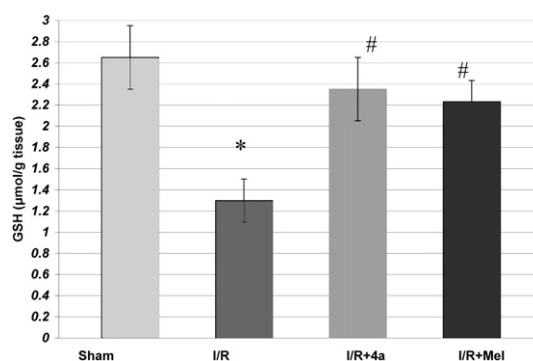
Compd.	Dose (mmol/kg)	Edema weight (X ± SD mg)	Inhibition (%)
NS		3.28 ± 0.49	
4a	0.15	1.29 ± 0.35 ^a	60.7
	0.10	1.65 ± 0.51 ^a	49.6
	0.05	2.01 ± 0.48 ^b	38.7
4e	0.15	1.55 ± 0.43 ^a	52.7
	0.10	1.81 ± 0.38 ^a	44.8
	0.05	2.21 ± 0.47	32.6
4k	0.15	1.47 ± 0.27 ^a	55.2
	0.10	1.79 ± 0.54 ^a	45.4
	0.05	2.35 ± 0.43	28.3
4o	0.15	1.61 ± 0.32 ^a	50.9
	0.10	2.20 ± 0.43	32.9
	0.05	2.75 ± 0.66	16.2
4p	0.15	1.41 ± 0.49 ^a	57.0
	0.10	2.41 ± 0.58	26.5
	0.05	2.91 ± 0.67	11.3

NS = vehicle; n = 10.

^a Compared to NS, P < 0.01.^b Compared to NS, P < 0.05.

2. Synthesis of β-carboline-tripeptide conjugates

Starting from optically active L-tryptophan, compound **1** was synthesized via the Pictet–Spengler reaction, and then subjected to protection. The *t*-butyloxycarbonyl (Boc) group has been widely used as a protecting group of various amino groups because of the mild deprotection condition. Treatment of compound **1** with

**Fig. 1.** MDA activities (nmol/g tissue) in the intestinal tissue of sham, ischemia/reperfusion (I/R), I/R + **4a** and I/R + melatonin groups. *: Compared with the sham group, P < 0.01; #: compared with the I/R group, P < 0.01; n = 8.**Fig. 2.** GSH levels (μmol/g tissue) in the intestinal tissue of sham, ischemia/reperfusion (I/R), I/R + **4a** and I/R + melatonin groups. *: Compared with the sham group, P < 0.01; #: Compared with the I/R group, P < 0.01; n = 8.

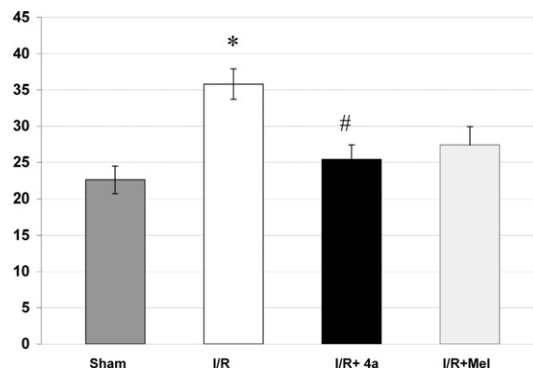
t-butyloxycarbonyl azide leads to selective acylation of the amino group. Subsequently, compound **2** coupled with tripeptides to generate a series of the key intermediates **3a–r**. After deprotection, the desired β-carboline-tripeptide conjugates **4a–r** can be readily prepared (Scheme 1).

3. Biological results and discussion

3.1. In vivo oral analgesic activities of **4a–r**

Analgesic activity was evaluated by the tail flick procedure [15,16]. The analgesic capacity was expressed by the pain threshold variation, defined as the difference of pain threshold after drug administration minus basic pain threshold/basic pain threshold.

All compounds were prescreened for analgesic activity at a dose of 0.15 mmol/kg. For each animal, pain thresholds were estimated at 30, 60, 120, 150 and 180 min following vehicle or drug administration. β-Carboline-tripeptide conjugates exhibited moderate to good analgesic activity, with compounds **4a,e,k,l,o,p** demonstrating especially good analgesic properties (Table 1). All pain thresholds were increased after 30 min, yet maximal pain thresholds occurred at different time points for various synthetic derivatives. For example, the maximal pain thresholds for **4a,c,e,h,m** were observed after 60 min, whereas for **4d,g,k,l,n,o,p** this value was 90 min, and for **4b,f,i,q,r**, 120 min post drug administration. The duration of the analgesic action of **4a,b,c,d,e,f,i,j** was 150 min, while the same value for **4k,l,m,n,o,p** was 180 min. We speculate that the physiological difference in analgesic activity is closely related to the tripeptide sequences of the β-carbolines.

**Fig. 3.** MPO activities (U/g) in the intestinal tissue of sham, ischemia/reperfusion (I/R), I/R + **4a** and I/R + melatonin groups. *: Compared with the sham group, P < 0.05; #: Compared with the I/R group, P < 0.05; n = 8.

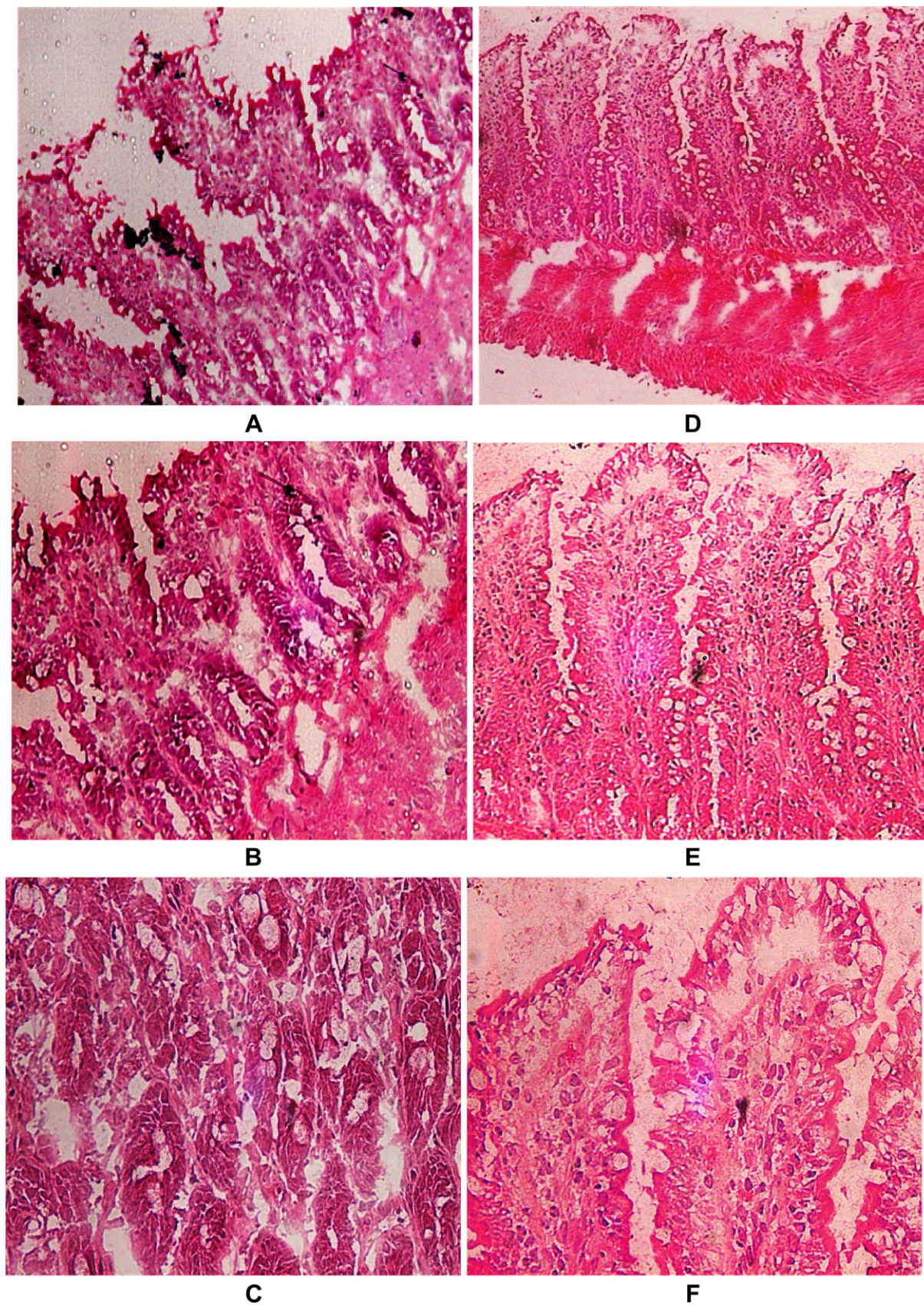


Fig. 4. Representative photomicrographs of histological sections of small intestine. (A)–(C): Representative tissue sections were taken from the rats exposed to ischemia/reperfusion; (D)–(F): tissues sections were taken from ischemia/reperfusion + (20 mg/kg) treated rats. Tissue sections were stained with H&E (hematoxylin and eosin). Magnification: (A, D) $\times 100$; (B, E) $\times 200$; (C, F) $\times 400$.

Table 5
Molecular dynamic simulation results.

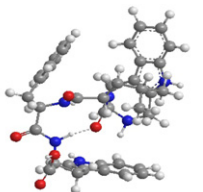
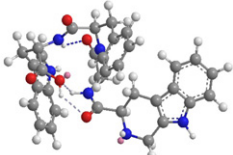
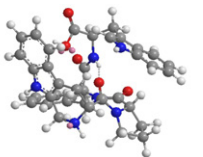
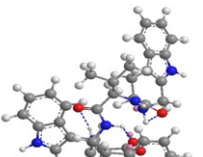
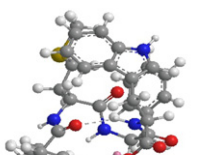
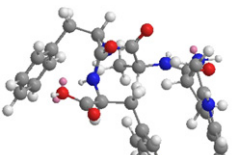
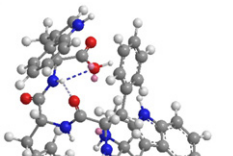
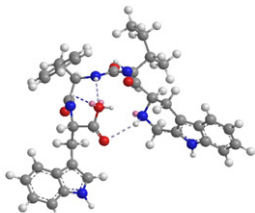
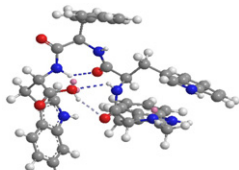
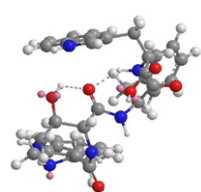
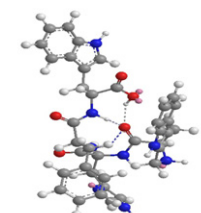
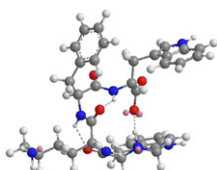
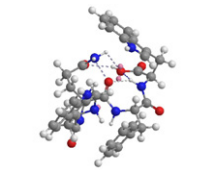
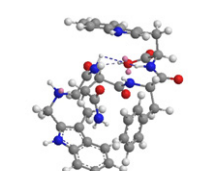
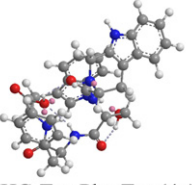
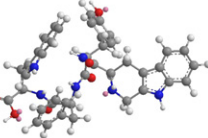
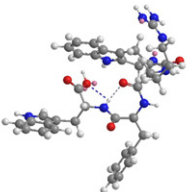
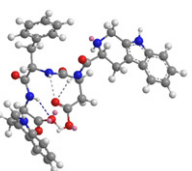
Predicted lowest energy conformations	E_{HOMO} (eV)	Distance between O and H (Å)
	-8.029	O(15)–H(65): 2.060 O(21)–H(76): 3.144
THC-Leu-Phe-Trp (4a)		
	-7.454	H(71)–O(15): 2.160 O(32)–H(57): 2.252 H(62)–O(45): 2.119
THC-Gly-Phe-Trp (4b)		
	-9.098	O(15)–H(64): 2.060
THC-Pro-Phe-Trp (4c)		
	-9.073	O(46)–H(64): 2.153 O(31)–H(60): 2.346 O(15)–H(56): 2.491
THC-Val-Phe-Trp (4d)		
	-8.204	O(15)–H(65): 2.104
THC-Ala-Phe-Trp (4e)		
	-9.856	None
THC-Phe-Phe-Trp (4f)		
	-10.091	O(46)–H(68): 2.024 O(31)–H(68): 2.262
THC-Ile-Phe-Trp (4g)		

Table 5 (continued)

Predicted lowest energy conformations	E_{HOMO} (eV)	Distance between O and H (Å)
	-9.977	O(32)–H(57): 2.315A O(31)–H(61): 2.419 O(31)–H(65): 2.129A
THC-Trp-Phe-Trp (4h)		
	-9.911	O(15)–H(80): 2.109 O(31)–H(87): 2.201 O(46)–H(71): 2.133
THC-Thr-Phe-Trp (4i)		
	-10.049	O(41)–H(64): 2.008 O(41)–H(78): 1.848
THC-His-Phe-Trp (4j)		
	-8.954	O(15)–H(67): 2.221 O(15)–H(63): 1.846 O(15)–H(71): 2.035
THC-Lys-Phe-Trp (4k)		
	-9.164	O(26)–H(58): 2.036 O(15)–H(62): 2.021 O(46)–H(66): 2.005
THC-Gln-Phe-Trp (4l)		
	-10.307	O(50)–H(70): 2.118 O(46)–H(89): 2.076 O(26)–H(66): 2.291 O(26)–H(88): 2.276
THC-Asn-Phe-Trp (4m)		
	-14.2209	O(15)–H(69): 2.246 O(26)–H(65): 2.235 O(26)–H(81): 2.708
THC-Ser-Phe-Trp (4n)		

(continued on next page)

Table 5 (continued)

Predicted lowest energy conformations	E_{HOMO} (eV)	Distance between O and H (Å)
 THC-Tyr-Phe-Trp (4o)	-8.989	O(15)–H(67): 2.143 O(46)–H(83): 1.858 O(26)–H(59): 2.224
 THC-Arg-Phe-Trp (4p)	-8.630	None
 THC-Asp-Phe-Trp (4q)	-10.052	O(46)–H(68): 2.077 O(26)–H(68): 2.180
 THC-Glu-Phe-Trp (4r)	-10.192	O(26)–H(65): 2.288 O(49)–H(81): 2.140 O(49)–H(61): 2.094

THC-: N-(3S-1,2,3,4-Tetrahydro-β-carboline-3-carboxyl)-.

3.2. Dose-dependency of analgesic activity for **4a** and **4k**

To investigate dose effects, the most active species (**4a,k**) were examined for dose-dependency of analgesia. Mice were administered 0.15, 0.10 and 0.05 mmol/kg of **4a,k** orally (Table 2). We observed a clear correlation between the amount of drug, and even at 0.05 mmol/kg, the analgesic activities of compounds **4a,k** was still measurable. Of interest, L-tryptophan, and the precursor peptides of **4a,k** (Leu-Phe-Trp and Lys-Phe-Trp), all possess analgesic activities, further suggesting that the analgesic activities of β-carboline-tripeptide conjugates **4a,k** might be due in part to the amino acid moieties or their downstream metabolites.

3.3. Anti-inflammatory activities of **4a–r**

All compounds were evaluated for anti-inflammatory capacity in a xylene-induced ear edema model [16]. Briefly, this *in vivo* assay involves oral administration of test compounds in 0.5% carboxymethyl cellulose (CMC) suspension. Each compound was initially tested at 0.15 mmol/kg, and all revealed significant protection against xylene-induced inflammation (Table 3), suggesting potent anti-inflammatory capacity. Since compounds (**4a,e,k,o,p**) exhibit good analgesic activities in the tail flick assay and superior anti-inflammatory activities in the xylene-induced ear edema model, these compounds were then examined in the same assay at lower

doses to establish the detailed pharmacological activity profile. From Table 4, we noticed a dose-dependent anti-inflammatory response for **4a,e,k,o,p**.

3.4. Intestinal I/R injury

Acute mesenteric ischemia leading to ischemic damage represents a serious clinical complication. During I/R, there are complex interactions between endothelial activation, inflammatory cell recruitment and production of reactive oxygen species. In addition, I/R injury induces the transport of proinflammatory molecules into the systemic circulation, promoting additional systemic inflammation. Based upon the analgesic and anti-inflammatory activities of **4a**, we characterized the effects of this compound on intestinal I/R injury in this model.

3.4.1. Effect of **4a** on lipid peroxidation monitored via malondialdehyde (MDA) and glutathione (GSH) analyses

Lipid peroxidation-induced oxidative stress is one cause of intestinal I/R, linked to membrane lipid composition. Accordingly, to assess intestinal lipid peroxidation and antioxidant defenses, malondialdehyde (MDA) and glutathione (GSH) levels were quantified in intestinal samples. MDA, an end-product of membrane lipid peroxidation, is a generally accepted surrogate biomarker of lipid peroxidation. MDA levels were determined following Beuge's method [18], while glutathione (GSH; a specific marker for protein oxidative damage) was determined using Beutler's method [19] (Fig. 1).

I/R significantly elevated MDA levels as compared to the sham group, suggesting that ROS-induced lipid peroxidation was underway in rat ileum. Conversely, **4a** intervention significantly attenuated this effect, likely due to the free radical scavenging capacity of this compound.

Reduced glutathione (GSH) is a tripeptide of glutamine, L-cysteine, and glycine and an endogenous antioxidant that reacts with various free radicals. Oxidation of GSH leads to a disulfide bridge (glutathione disulfide; GSSG) that can be re-reduced to generate free GSH. Intracellularly, a dynamic balance is maintained between GSH synthesis, consumption and oxidation. Typically, the GSH/GSSG ratio is 9:1 in a healthy cell, and measurement of this ratio is a useful estimator of intracellular oxidative stress [20]. We observed GSH during reperfusion (Fig. 2), and this effect was reversed via intervention with **4a**.

3.4.2. Effect of **4a** on MPO (myeloperoxidase) activity

I/R induces an acute inflammatory response in which elevated vascular permeability and increased adherence and emigration of leukocytes occurs. Neutrophils initially attach to the damaged vascular endothelium and accrue in the same vascular bed, and they are subsequently activated by proinflammatory cytokines and tissue infiltration. Accordingly, activated neutrophils represent an important factor in reperfused intestinal tissue injury [22,23]. Myeloperoxidase (MPO), the most abundant protein in neutrophils, is the focus of inflammatory pathologies. MPO assay is routinely measured as an index of neutrophil infiltration and a marker for acute inflammation when polymorphonuclear cell infiltration occurred [21]. We observed that MPO activity significantly increased after 3 h of reperfusion (Fig. 3), reflecting neutrophil infiltration, and this effect was again significantly attenuated in the presence of **4a**.

3.4.3. Histological analysis

We observed severe mucosal damage consistent with ischemic injury, ranging from vacuolation of villus tips to denuded villi and mucosal ulceration in the intestinal I/R group (Fig. 4A–C).

Characteristic features included marked congestion, hemorrhage, desquamation of villum epithelium and inflammatory cell infiltration, as well as the presence of crypts and shortening of the villi. We found mucosal damage on some of the surface epithelium, in addition to extension of the sub-epithelial space with moderate to massive epithelial lifting. Intervention with **4a** significantly reversed these findings, with only mild mucosal damage and minimal focal denudations of the villi epithelium (Fig. 4D–F).

3.5. Molecular dynamic simulation

The electron ionization energy is a quantitative descriptor of the capacity of a compound to scavenge oxidants. The ionization energy from the highest occupied molecular orbital (HOMO) can be estimated by Koopmans theorem, with reasonable accuracy [24]. The HOMO energy is often employed as a primary descriptor of radical scavenging/antioxidant activity [25]. The high HOMO energy of our indole β -carboline derivatives highlights their electron-donating potential and coordination capacities, suggesting they may serve as metal ion coordinators and subsequently as inhibitors of ion-catalyzed oxidation processes (Table 5).

Generally, the higher the HOMO energy, the more potent the antioxidant activity. The HOMO energy of the endogenous antioxidant melatonin is -10.425 eV. In comparison, the HOMO energy of compounds **4a,b,e,k,o,p** were -8.029 eV, -7.454 eV, -8.204 eV, -8.954 eV, -8.989 eV and -8.630 eV, respectively. Accordingly, **4a,b,e,k,o,p** should possess higher radical trapping potentials than melatonin. Moreover, the high positive charge of the hydrogen atoms connected to the nitrogen atoms in the indole β -carboline cation radical reflect significant N–H acidity, and these readily released protons may help to facilitate the scavenging process.

3.6. Conclusion

In the present study, we have synthesized a series of new β -carboline-tripeptide conjugates, and examined their anti-inflammatory and analgesic activities. In light of potent analgesic and anti-inflammatory activity, compound **4a** was further evaluated in an intestinal ischemia/reperfusion injury animal model and found to attenuate the structural and functional damage observed in intestinal I/R. We speculate that these protective effects might relate to reduced inflammation and an inhibition of lipid peroxidation.

4. Experimental

4.1. General

All chemicals were purchased from Sigma Aldrich. Unless otherwise stated, all reactions were run under a nitrogen atmosphere (1 bar). Chromatography was performed on Qingdao silica gel H (230–400mesh). The purity ($>97\%$) of the intermediates and the final products was confirmed via both TLC (Merck silica gel plates, type 60 F254, 0.25 mm layer thickness) and HPLC (Waters, C18 column 4.6 mm \times 150 mm). NMR spectra were recorded on a Bruker Advance 500 spectrometer. FAB-MS was determined by VG-ZAB-MS high resolution GC/MS/DS and HP ES-5989x.

4.2. Synthesis of β -carboline-tripeptide conjugates **4a–r**

4.2.1. 3S-1,2,3,4-Tetrahydro- β -carboline-3-carboxylic acid (**1**)

L-Tryptophan (5.0 g; 24.5 mmol) was supplemented with 25 mL of H_2SO_4 (1 mol/L), 80 mL of water, and 8 mL of formaldehyde (36–38%) were added. The reaction mixture was stirred at room temperature for 2 h and adjusted to pH 6–7 with concentrated

ammonia. The mixture was maintained at 0°C for 12 h and the precipitate was collected by filtration. After re-crystallization, 3.97 g (75%) of product was obtained as a colorless powder. Mp: $280\text{--}282^\circ\text{C}$. EI/MS: 217 $[\text{M} + \text{H}]^+$; IR (KBr): 3450, 3200, 3000, 2950, 2850, 1700, 1601, 1452, 1070, 900 cm^{-1} ; ^1H NMR (BHSC-500, DMSO- d_6): δ/ppm = 10.99 (s, 1H), 9.89 (s, 1H), 7.30 (t, $J = 7.5$ Hz, 1H), 7.22 (t, $J = 8.0$ Hz, 1H), 7.01 (d, $J = 8.0$ Hz, 1H), 6.81 (d, $J = 7.5$ Hz, 1H), 4.01 (t, $J = 4.8$ Hz, 1H), 3.75 (dd, $J = 10.5$ Hz, $J = 5.0$ Hz, 1H), 3.64 (dd, $J = 10.5$ Hz, $J = 2.4$ Hz, 1H), 2.91 (d, $J = 10.5$ Hz, 2H), 2.86 (s, 1H). Anal. Calcd for $\text{C}_{12}\text{H}_{12}\text{N}_2\text{O}_2$: C, 66.65; H, 5.59; N, 12.96. Found: C, 66.45; H, 5.72; N, 12.79.

4.2.2. N-Boc-3S-1,2,3,4-Tetrahydro- β -carboline-3-carboxylic acid (**2**)

A suspension of 1.1 g (5.0 mmol) of **1** in 15 mL DMF and 1.4 mL of triethylamine was vigorously stirred at room temperature, and supplemented with 1.1 g (7.7 mmol) of Boc- N_3 over a 30 min period. The reaction mixture was stirred at room temperature for 24 h and then at 40°C for 80 h. Citrate solution (5 mL; 20%) was then added and the solution extracted with ethyl acetate (3×30 mL). Combined ethyl acetate fractions were dried over anhydrous MgSO_4 . The filtrate was dried by evaporation after removal of MgSO_4 . The residue was crystallized in CHCl_3 to yield 1.20 g (76%) of product. Mp: $165\text{--}170^\circ\text{C}$. TOF/MS: 317 $[\text{M} + \text{H}]^+$, 339 $[\text{M} + \text{Na}]^+$, 355 $[\text{M} + \text{K}]^+$; IR (KBr): 3452, 3205, 3001, 2952, 2848, 1705, 1645, 1600, 1450, 1072, 901 cm^{-1} ; ^1H NMR (BHSC-500, DMSO- d_6): δ/ppm = 10.87 (s, 1H), 9.86 (s, 1H), 7.32 (t, $J = 7.6$ Hz, 1H), 7.21 (t, $J = 7.9$ Hz, 1H), 7.00 (d, $J = 7.9$ Hz, 1H), 6.84 (t, $J = 7.6$ Hz, 1H), 4.84 (t, $J = 5.0$ Hz, 1H), 4.20 (dd, $J = 10.2$ Hz, $J = 4.8$ Hz, 1H), 3.98 (dd, $J = 10.2$ Hz, $J = 3.2$ Hz, 1H), 2.93 (d, $J = 10.2$ Hz, 2H), 1.46 (s, 9H). Anal. Calcd for $\text{C}_{17}\text{H}_{20}\text{N}_2\text{O}_4$: C, 64.54; H, 6.37; N, 8.86. Found: C, 64.41; H, 6.25; N, 8.74.

4.2.3. Boc-Phe-Trp-OCH₃

HOBt (250 mg; 1.75 mmol) and dicyclohexylcarbodiimide (400 mg; 1.95 mmol) were added to a solution of 465 mg (1.75 mmol) Boc-Phe-OH in THF (15 mL). After stirring for 1 h at 0°C , 490 mg (1.95 mmol) HCl-Trp-OCH₃ was added and the pH adjusted to 8–9 with NMM. The reaction mixture was stirred overnight at room temperature. Precipitated dicyclohexylurea was removed by filtration. The filtrate was evaporated under reduced pressure, and the residue dissolved in 50 mL of ethyl acetate. The solution was washed with saturated NaHCO_3 (10 mL \times 3), 5% KHSO_4 (10 mL \times 3) and saturated sodium chloride, and the organic phase separated and dried over anhydrous sodium sulfate. Following filtration and evaporation under reduced pressure, purification by chromatography provided the final product. Mp: $165\text{--}166^\circ\text{C}$. ESI-MS (m/e) 466 $[\text{M} + \text{H}]^+$; ^1H NMR (500 Hz, CDCl_3) δ/ppm = 10.78 (s, 1H), 8.15 (s, 1H), 7.40 (d, $J = 7.0$ Hz, 1H), 7.35 (d, $J = 8.0$ Hz, 1H), 7.30–7.23 (m, 5H), 7.20 (t, $J = 7.5$ Hz, 1H, 1H), 7.09 (t, $J = 7.5$ Hz, 1H), 6.90 (s, 1H), 6.38 (d, $J = 5.5$ Hz, 1H), 4.90 (m, 1H), 4.36 (m, 1H), 3.65 (s, 3H), 3.28 (m, 2H), 3.06–3.04 (m, 2H), 1.39 (s, 9H). ^{13}C NMR (125 Hz, CDCl_3) δ/ppm = 171.75, 170.77, 155.25, 136.59, 136.08, 129.43, 128.62, 127.53, 126.93, 122.26, 119.69, 118.49, 111.30, 109.79, 80.09, 55.68, 52.99, 52.31, 38.36, 28.21, 27.70.

4.2.4. HCl-Phe-Trp-OCH₃

Boc-Phe-Trp-OCH₃ (0.2 mmol) in 2 mL of hydrogen chloride in ethyl acetate (4 mol/L) was stirred for 3 h at room temperature, and solvent was removed by evaporation. The residue was dissolved in 10 mL of ethyl acetate, and the solution again evaporated to dryness. The resulting solid was used for the coupling reaction without further purification. Mp: $176\text{--}178^\circ\text{C}$. ESI-MS (m/e) 366 $[\text{M} + \text{H}]^+$; ^1H NMR (500 Hz, DMSO- d_6) δ/ppm = 11.02 (s, 1H), 9.25 (d, $J = 7.5$ Hz, 1H), 8.33 (s, 2H), 7.50 (d, $J = 8.0$ Hz, 1H), 7.37 (d, $J = 8.0$ Hz, 1H), 7.33–7.25 (m, 6H), 7.07 (t, $J = 7.5$ Hz, 1H), 7.01

(t, $J = 7.5$ Hz, 1H), 4.59 (m, 1H), 4.13 (m, 1H), 3.25–3.19 (m, 3H), 3.02 (dd, $J = 7.5$ Hz, $J = 14.0$ Hz, 1H). ^{13}C NMR (125 Hz, DMSO- d_6) δ /ppm = 171.39, 170.41, 155.41, 136.71, 136.28, 129.32, 128.71, 127.02, 122.79, 122.23, 119.65, 118.66, 111.27, 56.29, 52.08, 38.73, 26.30.

4.2.5. Boc–Leu–Phe–Trp–OCH₃ (a)

HCl·Phe–Trp–OCH₃ (603 mg; 1.5 mmol) and Boc–Leu–OH (346 mg; 1.5 mmol) were combined to derive the coupled compound as a colorless solid (521 mg; 60% yield). Mp: 154–156 °C. ESI-MS (m/e) 579 [M + H]⁺; ^1H NMR (500 Hz, DMSO- d_6) δ /ppm = 10.88 (s, 1H), 8.52 (d, $J = 7.5$ Hz, 1H), 7.74 (d, $J = 8.5$ Hz, 1H), 7.49 (d, $J = 8.0$ Hz, 1H), 7.35 (d, $J = 8.0$ Hz, 1H), 7.25–7.18 (m, 5H), 7.16 (s, 1H), 7.08 (t, $J = 7.5$ Hz, 1H), 6.90 (d, $J = 9.0$ Hz, 1H), 4.63 (m, 1H), 4.53 (m, 1H), 3.88 (m, 1H), 3.56 (s, 3H), 3.16 (dd, $J = 6.5$ Hz, $J = 14.5$ Hz, 1H), 3.09 (dd, $J = 7.5$ Hz, $J = 14.5$ Hz, 1H), 3.00 ($J = 4.5$ Hz, $J = 13.5$ Hz, 1H), 2.79 (dd, $J = 4.5$ Hz, $J = 13.5$ Hz, 1H), 1.46 (m, 1H), 1.37 (s, 9H), 1.30 (m, 2H), 0.825 (d, $J = 7.0$ Hz, 3H), 0.79 (d, $J = 7.0$ Hz, 3H). ^{13}C NMR (125 Hz, DMSO- d_6) δ /ppm = 172.54, 172.45, 171.52, 155.63, 137.87, 136.55, 129.79, 128.36, 127.53, 126.65, 124.16, 118.89, 118.41, 111.90, 109.55, 78.57, 53.62, 53.49, 52.26, 41.33, 38.26, 28.63, 27.54, 24.64, 23.34, 21.98.

4.2.6. Boc–Gly–Phe–Trp–OCH₃ (b)

HCl·Phe–Trp–OCH₃ (804 mg; 2.0 mmol) and Boc–Gly–OH (350 mg; 1.5 mmol) were combined to derive the coupled product as a colorless solid (635 mg; 81% yield). Mp: 84–86 °C. ESI-MS (m/e) 523 [M + H]⁺; ^1H NMR (500 Hz, DMSO- d_6) δ /ppm = 10.89 (s, 1H), 8.54 (d, $J = 7.5$ Hz, 1H), 7.90 (d, $J = 8.5$ Hz, 1H), 7.50 (d, $J = 8.0$ Hz, 1H), 7.36 (d, $J = 8.0$ Hz, 1H), 7.29–7.20 (m, 5H), 7.19 (s, 1H), 7.10 (t, $J = 7.0$ Hz, 1H), 7.07 (t, $J = 7.0$ Hz, 1H), 6.92 (t, $J = 6.0$ Hz, 1H), 4.60 (m, 1H), 4.54 (m, 1H), 3.55 (s, 1H), 3.39 (s, 2H), 3.24 ($J = 7.5$ Hz, $J = 15.0$ Hz, 1H), 3.09 (dd, $J = 7.5$ Hz, $J = 15.0$ Hz, 1H), 2.95 (dd, $J = 4.5$ Hz, $J = 11.0$ Hz, 1H), 2.68 (dd, $J = 7.5$ Hz, $J = 11.0$ Hz, 1H), 1.38 (s, 9H). ^{13}C NMR (125 Hz, DMSO- d_6) δ /ppm = 172.50, 171.50, 169.47, 156.21, 137.99, 136.55, 129.70, 128.46, 127.52, 126.71, 124.23, 121.45, 118.91, 118.42, 111.91, 109.63, 78.56, 53.82, 53.56, 52.28, 43.55, 38.16, 28.65, 27.51.

4.2.7. Boc–Pro–Phe–Trp–OCH₃ (c)

HCl·Phe–Trp–OCH₃ (603 mg; 1.5 mmol) and Boc–Pro–OH (323 mg; 1.5 mmol) were combined to yield coupled product as a colorless solid (632 mg; 75% yield). Mp: 102–103 °C. ESI-MS (m/e) 562 [M + H]⁺; ^1H NMR (500 Hz, DMSO- d_6) δ /ppm = 10.91 (s, 1H), 8.53 (d, $J = 7.0$ Hz, 1H), 7.82 (d, $J = 8.5$ Hz, 1H), 7.49 (d, $J = 8.0$ Hz, 1H), 7.35 (d, $J = 8.0$ Hz, 1H), 7.28–7.23 (m, 5H), 7.19 (s, 1H), 7.08 (t, $J = 7.5$ Hz, 1H), 7.00 (t, $J = 7.5$ Hz, 1H), 4.64 (m, 1H), 4.57 (m, 1H), 4.00 (m, 1H), 3.56 (s, 3H), 3.41–3.32 (m, 2H), 3.24–3.16 (m, 2H), 3.10 (dd, $J = 8.0$ Hz, $J = 15.0$ Hz, 1H), 3.00 (dd, $J = 8.0$ Hz, $J = 15.0$ Hz, 1H), 2.00 (m, 1H), 1.67–1.60 (m, 3H), 1.13 (s, 9H). ^{13}C NMR (125 Hz, DMSO- d_6) δ /ppm = 172.54, 172.25, 153.80, 138.19, 136.57, 129.63, 128.40, 127.53, 126.67, 124.10, 121.44, 118.88, 118.41, 111.90, 109.62, 78.82, 60.07, 53.94, 53.57, 52.27, 46.92, 38.06, 29.87, 29.47, 28.61, 23.37.

4.2.8. Boc–Val–Phe–Trp–OCH₃ (d)

HCl·Phe–Trp–OCH₃ (803 mg; 2.0 mmol) and Boc–Val–OH (434 mg; 2.0 mmol) were combined to derive the end-product as a colorless solid (813 mg; 72% yield). Mp: 179–180 °C. ESI-MS (m/e) 565 [M + H]⁺; ^1H NMR (500 Hz, DMSO- d_6) δ /ppm = 10.59 (s, 1H), 8.51 (d, $J = 7.0$ Hz, 1H), 7.90 (d, $J = 8.5$ Hz, 1H), 7.48 (d, $J = 8.0$ Hz, 1H), 7.35 (d, $J = 8.0$ Hz, 1H), 7.24–7.16 (m, 6H), 7.07 (t, $J = 7.5$ Hz, 1H), 7.00 (t, $J = 5.0$ Hz, 1H), 6.65 (d, $J = 9.0$ Hz, 1H), 4.66 (m, 1H), 4.53 (m, 1H), 3.73 (m, 1H), 3.55 (s, 3H), 3.15 (dd, $J = 6.0$ Hz, $J = 14.5$ Hz, 1H), 3.09 (dd, $J = 7.5$ Hz, $J = 14.5$ Hz, 1H), 2.99 (dd, $J = 4.5$ Hz, $J = 13.5$ Hz, 1H), 2.77 (dd, $J = 9.5$ Hz, $J = 13.5$ Hz, 1H), 1.80 (m, 1H), 1.38 (s, 9H), 0.68 (dd, $J = 6.5$ Hz, $J = 17.5$ Hz, 6H). ^{13}C NMR (125 Hz, DMSO- d_6) δ /ppm = 172.44, 171.66, 171.45, 155.74, 138.01, 136.55, 129.69, 128.42,

127.52, 126.67, 124.16, 121.43, 118.88, 118.41, 111.89, 109.53, 78.53, 60.37, 53.70, 53.57, 52.26, 38.24, 31.00, 28.63, 27.52, 19.55, 18.52.

4.2.9. Boc–Ala–Phe–Trp–OCH₃ (e)

HCl·Phe–Trp–OCH₃ (803 mg; 2.0 mmol) and Boc–Ala–OH (378 mg; 2.0 mmol) were combined to derive the coupled compound as a colorless solid (967 mg; 90% yield). Mp: 96–98 °C. ESI-MS (m/e) 537 [M + H]⁺; ^1H NMR (500 Hz, DMSO- d_6) δ /ppm = 11.45 (s, 1H), 8.54 (d, $J = 7.0$ Hz, 1H), 7.91 (d, $J = 8.0$ Hz, 1H), 7.50 (d, $J = 8.0$ Hz, 1H), 7.35 (d, $J = 8.5$ Hz, 1H), 7.26–7.17 (m, 6H), 7.08 (t, $J = 7.5$ Hz, 1H), 7.00 (t, $J = 7.5$ Hz, 1H), 6.92 (t, $J = 6.5$ Hz, 1H), 4.60 (m, 1H), 3.57 (s, 3H), 3.46 (m, 1H), 3.18 (dd, $J = 6.0$ Hz, $J = 14.5$ Hz, 1H), 3.09 (dd, $J = 7.5$ Hz, $J = 14.5$ Hz, 1H), 2.99 (dd, $J = 4.5$ Hz, $J = 4.0$ Hz, 1H), 2.77 (dd, $J = 9.5$ Hz, $J = 14.0$ Hz, 1H), 1.38 (s, 9H), 1.25 (d, $J = 10.0$ Hz, 3H). ^{13}C NMR (125 Hz, DMSO- d_6) δ /ppm = 172.51, 171.52, 169.47, 156.21, 137.99, 136.54, 129.71, 128.46, 127.51, 126.71, 124.23, 121.45, 118.91, 118.42, 111.91, 109.62, 78.54, 53.81, 53.56, 52.29, 43.52, 38.16, 28.65, 27.50, 18.88.

4.2.10. Boc–Phe–Phe–Trp–OCH₃ (f)

HCl·Phe–Trp–OCH₃ (803 mg; 2.0 mmol) and Boc–Ile–OH (530 mg; 2.0 mmol) were coupled to derive a yellow solid (1042 mg; 85% yield). Mp: 90–91 °C. ESI-MS (m/e) 613 [M + H]⁺; ^1H NMR (500 Hz, DMSO- d_6) δ /ppm = 10.90 (s, 1H), 8.57 (d, $J = 7.5$ Hz, 1H), 8.27 (d, $J = 8.5$ Hz, 1H), 7.55 (d, $J = 7.5$ Hz, 1H), 7.35 (d, $J = 8.5$ Hz, 1H), 7.24–7.12 (m, 1H), 7.08 (t, $J = 7.5$ Hz, 1H), 7.0 (t, $J = 7.5$ Hz, 1H), 6.87 (d, $J = 8.0$ Hz, 1H), 4.65 (m, 1H), 4.55 (m, 1H), 4.12 (m, 1H), 3.58 (s, 3H), 3.18 (dd, $J = 6.0$ Hz, $J = 15.0$ Hz, 1H), 3.10 (dd, $J = 7.5$ Hz, $J = 15.0$ Hz, 1H), 3.03 (dd, $J = 5.0$ Hz, $J = 14.0$ Hz, 1H), 2.82 (dd, $J = 9.5$ Hz, $J = 14.0$ Hz, 2H), 2.62 (dd, $J = 10.5$ Hz, $J = 14.0$ Hz, 1H), 1.30 (s, 9H). ^{13}C NMR (125 Hz, DMSO- d_6) δ /ppm = 172.47, 171.79, 171.53, 155.51, 138.56, 137.90, 136.54, 129.72, 129.59, 128.46, 128.41, 127.53, 126.74, 126.56, 124.23, 121.44, 118.90, 118.42, 111.90, 109.56, 78.57, 56.24, 53.79, 53.61, 52.29, 38.29, 37.98, 28.56, 27.54.

4.2.11. Boc–Ile–Phe–Trp–OCH₃ (g)

HCl·Phe–Trp–OCH₃ (1003 mg; 2.5 mmol) and Boc–Phe–OH (577 mg; 2.5 mmol) were combined to derive the end-product as a colorless solid (1164 mg; 81% yield). Mp: 189–190 °C. ESI-MS (m/e) 576 [M + H]⁺; ^1H NMR (500 Hz, DMSO- d_6) δ /ppm = 10.88 (s, 1H), 8.48 (d, $J = 7.5$ Hz, 1H), 7.89 (d, $J = 8.5$ Hz, 1H), 7.48 (d, $J = 8.0$ Hz, 1H), 7.35 (d, $J = 8.0$ Hz, 1H), 7.24–7.16 (m, 6H), 7.08 (t, $J = 7.5$ Hz, 1H), 7.00 (t, $J = 7.5$ Hz, 1H), 6.69 (d, $J = 9.0$ Hz, 1H), 4.66 (m, 1H), 4.52 (m, 1H), 3.76 (m, 1H), 3.54 (s, 3H), 3.15 (dd, $J = 6.5$ Hz, $J = 14.5$ Hz, 1H), 3.09 (dd, $J = 7.5$ Hz, $J = 14.5$ Hz, 1H), 2.99 (dd, $J = 4.5$ Hz, $J = 14.0$ Hz, 1H), 2.78 (dd, $J = 10.0$ Hz, 14.0 Hz, 1H), 1.55 (m, 1H), 1.38 (s, 9H), 1.28–1.21 (m, 2H), 0.73 (t, $J = 7.5$ Hz, 3H), 0.60 (d, $J = 7.0$ Hz, 3H). ^{13}C NMR (125 Hz, DMSO- d_6) δ /ppm = 172.42, 171.62, 171.49, 155.66, 138.00, 136.56, 129.69, 128.39, 127.53, 126.65, 124.15, 121.43, 118.41, 111.89, 78.54, 59.46, 53.67, 53.59, 52.24, 38.24, 37.05, 28.64, 27.55, 24.69, 15.59, 11.31.

4.2.12. Boc–Trp–Phe–Trp–OCH₃ (h)

HCl·Phe–Trp–OCH₃ (804 mg; 2.0 mmol) and Boc–Trp–OH (608 mg; 2.0 mmol) were combined to derive the targeted product as a colorless solid (723 mg; 78% yield). Mp: 101–104 °C. ESI-MS (m/e) 465 [M + H]⁺; ^1H NMR (500 Hz, DMSO- d_6) δ /ppm = 10.90 (s, 1H), 10.78 (s, 1H), 8.57 (d, $J = 7.0$ Hz, 1H), 7.94 (d, $J = 8.5$ Hz, 1H), 7.54 (d, $J = 8.0$ Hz, 1H), 7.50 (d, $J = 8.0$ Hz, 1H), 7.35 (d, $J = 8.0$ Hz, 1H), 7.32 (d, $J = 8.0$ Hz, 1H), 7.30–7.18 (m, 6H), 7.01–6.96 (m, 5H), 6.79 (d, $J = 8.0$ Hz, 1H), 4.67 (m, 1H), 4.57 (m, 1H), 4.16 (m, 1H), 3.57 (s, 1H), 3.17 (dd, $J = 8.5$ Hz, $J = 14.5$ Hz, 1H), 3.11 (dd, $J = 7.5$ Hz, $J = 14.5$ Hz, 1H), 3.03 (dd, $J = 5.0$ Hz, $J = 14.0$ Hz, 1H), 2.93 (dd, $J = 4.5$ Hz, $J = 15.0$ Hz, 1H), 2.86–2.78 (m, 2H), 1.29 (s, 9H); ^{13}C NMR (125 Hz, DMSO- d_6) δ /ppm = 172.47, 172.05, 171.55, 155.53, 137.92, 136.56, 136.50, 129.85, 128.43, 127.85, 127.56, 126.72, 124.21, 123.92,

121.45, 121.26, 118.91, 118.87, 118.62, 118.44, 111.91, 111.71, 110.76, 109.57, 78.59, 55.86, 53.73, 53.66, 52.28, 38.32, 28.56, 28.24, 27.56.

4.2.13. Boc–Thr–Phe–Trp–OCH₃ (**i**)

HCl·Phe–Trp–OCH₃ (804 mg; 2.0 mmol) and Boc–Thr–OH (438 mg; 2.0 mmol) were combined to derive the end-product as a colorless solid (637 mg; 75% yield). Mp: 95–97 °C. ESI-MS (*m/e*) 567 [M + H]⁺; ¹H NMR (500 Hz, DMSO-*d*₆) δ/ppm = 10.87 (s, 1H), 8.50 (d, *J* = 7.0 Hz, 1H), 7.91 (d, *J* = 8.0 Hz, 1H), 7.48 (d, *J* = 8.0 Hz, 1H), 7.35 (d, *J* = 8.5 Hz, 1H), 7.24–7.16 (m, 6H), 7.08 (t, *J* = 7.5 Hz, 1H), 7.00 (t, 7.5 Hz, 1H), 6.38 (d, *J* = 8.0 Hz, 1H), 4.61 (m, 1H), 4.51 (m, 1H), 3.86–3.79 (m, 2H), 3.55 (s, 3H), 3.16 (dd, *J* = 6.5 Hz, *J* = 14.5 Hz, 1H), 3.07 (dd, *J* = 8.0 Hz, *J* = 14.5 Hz, 1H), 3.01 (dd, *J* = 4.5 Hz, *J* = 14.0 Hz, 1H), 2.79 (dd, *J* = 9.0 Hz, *J* = 13.5 Hz, 1H), 1.37 (s, 9H), 0.91 (d, *J* = 6.0 Hz, 3H). ¹³C NMR (125 Hz, DMSO-*d*₆) δ/ppm = 172.45, 171.44, 170.47, 155.73, 137.87, 136.55, 129.71, 128.45, 126.72, 124.01, 121.49, 118.94, 118.39, 111.93, 109.55, 78.85, 67.22, 60.50, 53.79, 53.68, 52.27, 37.94, 28.57, 27.50, 19.84.

4.2.14. Boc–His(Boc)–Phe–Trp–OCH₃ (**j**)

HCl·Phe–Trp–OCH₃ (804 mg; 2.0 mmol) and Boc–His(Boc)–OH (710 mg; 2.0 mmol) were combined to derive the end-product as a colorless solid (996 mg; 71% yield). Mp: 147–148 °C. ESI-MS (*m/e*) 703 [M + H]⁺; ¹H NMR (500 Hz, DMSO-*d*₆) δ/ppm = 10.90 (s, 1H), 8.58 (d, *J* = 7.5 Hz, 1H), 8.10 (s, 1H), 7.91 (d, *J* = 8.0 Hz, 1H), 7.48 (d, *J* = 8.0 Hz, 1H), 7.25–7.16 (m, 6H), 7.07 (t, *J* = 7.5 Hz, 1H), 6.99 (t, *J* = 7.5 Hz, 1H), 6.88 (d, *J* = 8.5 Hz, 1H), 4.61–4.53 (m, 2H), 4.16 (m, 1H), 3.56 (s, 3H), 3.17 (dd, *J* = 5.5 Hz, *J* = 14.5 Hz, 1H), 3.08 (dd, *J* = 7.5 Hz, *J* = 14.5 Hz, 1H), 3.00 (dd, *J* = 4.5 Hz, *J* = 14.0 Hz, 1H), 2.80 (dd, *J* = 9.5 Hz, *J* = 14.0 Hz, 1H), 2.74 (dd, *J* = 4.0 Hz, *J* = 15.0 Hz, 1H), 2.63 (dd, *J* = 9.5 Hz, *J* = 15.0 Hz, 1H), 1.54 (s, 9H), 1.33 (s, 9H). ¹³C NMR (125 Hz, DMSO-*d*₆) δ/ppm = 172.48, 171.45, 155.54, 147.15, 137.94, 137.07, 136.54, 129.77, 128.41, 127.54, 126.68, 124.16, 121.43, 118.89, 118.42, 114.61, 111.88, 109.56, 85.53, 78.71, 54.26, 53.85, 53.57, 52.28, 38.01, 31.10, 28.54, 27.82, 27.51.

4.2.15. Boc–Lys(Boc)–Phe–Trp–OCH₃ (**k**)

HCl·Phe–Trp–OCH₃ (1100 mg; 2.5 mmol) and Boc–Lys(Boc)–OH (865 mg; 2.5 mmol) were combined to derive the end-product as a yellow solid (1559 mg; 90% yield). Mp: 132–134 °C. ESI-MS (*m/e*) 694 [M + H]⁺; ¹H NMR (500 Hz, DMSO-*d*₆) δ/ppm = 10.88 (s, 1H), 8.50 (d, *J* = 7.5 Hz, 1H), 7.77 (d, *J* = 8.0 Hz, 1H), 7.48 (d, *J* = 8.0 Hz, 1H), 7.34 (d, *J* = 8.0 Hz, 1H), 7.25–7.16 (m, 6H), 7.08 (t, *J* = 7.5 Hz, 1H), 7.00 (t, *J* = 7.5 Hz, 1H), 6.83 (d, *J* = 8.0 Hz, 1H), 6.75 (t, *J* = 5.0 Hz, 1H), 4.62 (m, 1H), 4.54 (m, 1H), 3.80 (m, 1H), 3.56 (s, 3H), 3.16 (dd, *J* = 6.5 Hz, *J* = 15.0 Hz, 1H), 3.09 (dd, *J* = 7.5 Hz, *J* = 14.5 Hz, 1H), 2.99 (dd, *J* = 4.5 Hz, *J* = 13.5 Hz, 1H), 2.89–2.82 (m, 2H), 2.78 (dd, *J* = 4.0 Hz, *J* = 13.5 Hz, 1H), 1.38 (s, 9H), 1.37 (s, 9H), 1.31–1.25 (m, 2H), 1.21–1.18 (m, 4H). ¹³C NMR (125 Hz, DMSO-*d*₆) δ/ppm = 172.45, 172.27, 171.53, 156.03, 155.68, 137.89, 136.54, 129.77, 128.38, 127.54, 126.67, 124.16, 121.43, 118.89, 118.41, 111.89, 109.55, 78.58, 77.79, 55.06, 53.58, 52.26, 38.22, 32.16, 29.65, 28.75, 27.53, 23.22.

4.2.16. Boc–Gln–Phe–Trp–OCH₃ (**l**)

HCl·Phe–Trp–OCH₃ (804 mg; 2.0 mmol) and Boc–Thr–OH (438 mg; 2.0 mmol) were combined to derive the end-product as a colorless solid (771 mg; 65% yield). Mp: 193–194 °C. ESI-MS (*m/e*) 594 [M + H]⁺; ¹H NMR (500 Hz, DMSO-*d*₆) δ/ppm = 10.89 (s, 1H), 8.54 (d, *J* = 7.0 Hz, 1H), 7.87 (d, *J* = 8.0 Hz, 1H), 7.48 (d, *J* = 8.0 Hz, 1H), 7.45 (d, *J* = 8.0 Hz, 1H), 7.34–7.16 (m, 6H), 7.08 (t, *J* = 7.5 Hz, 1H), 7.00 (t, *J* = 7.5 Hz, 1H), 6.89 (d, *J* = 8.0 Hz, 1H), 6.81 (s, 2H), 4.60 (m, 1H), 4.54 (m, 1H), 3.87 (m, 1H), 3.56 (s, 3H), 3.17 (dd, *J* = 6.5 Hz, *J* = 15.0 Hz, 1H), 3.08 (dd, *J* = 7.5 Hz, *J* = 14.5 Hz, 1H), 2.99 (dd, *J* = 5.0 Hz, *J* = 14.0 Hz, 1H), 2.79 (dd, *J* = 9.0 Hz, *J* = 13.5 Hz, 1H), 2.11–2.00 (m, 2H), 1.74 (m, 1H), 1.62 (m, 1H), 1.37 (s, 9H). ¹³C NMR

(125 Hz, DMSO-*d*₆) δ/ppm = 174.46, 172.45, 171.97, 171.46, 155.66, 137.87, 136.54, 129.93, 128.42, 127.53, 126.69, 124.12, 121.44, 118.90, 118.41, 111.89, 109.63, 78.62, 54.53, 53.75, 53.52, 52.27, 38.23, 32.05, 28.64, 28.40, 27.48.

4.2.17. Boc–Asn–Phe–Trp–OCH₃ (**m**)

HCl·Phe–Trp–OCH₃ (600 mg; 1.5 mmol) and Boc–Asn–OH (350 mg; 1.5 mmol) were combined to derive the end-product as a yellow solid (773 mg; 89% yield). Mp: 184–185 °C. ESI-MS (*m/e*) 580 [M + H]⁺; ¹H NMR (500 Hz, DMSO-*d*₆) δ/ppm = 10.88 (s, 1H), 8.52 (d, *J* = 7.0 Hz, 1H), 7.82 (d, *J* = 8.0 Hz, 1H), 7.49 (d, *J* = 8.0 Hz, 1H), 7.35 (d, *J* = 8.0 Hz, 1H), 7.31 (s, 1H), 7.31–7.17 (m, 6H), 7.08 (t, *J* = 7.5 Hz, 1H), 7.00 (t, *J* = 7.5 Hz, 1H), 6.92 (d, *J* = 8.0 Hz, 2H), 4.55–4.50 (m, 2H), 4.23 (m, 1H), 3.56 (s, 3H), 3.17 (dd, *J* = 6.5 Hz, *J* = 14.5 Hz, 1H), 3.09 (dd, *J* = 7.5 Hz, *J* = 14.5 Hz, 1H), 2.95 (dd, *J* = 4.5 Hz, *J* = 14.0 Hz, 1H), 2.80 (dd, *J* = 8.5 Hz, *J* = 14.0 Hz, 1H), 2.41 (dd, *J* = 5.0 Hz, *J* = 15.0 Hz, 1H), 2.32 (dd, *J* = 8.0 Hz, *J* = 15.0 Hz, 1H), 1.37 (s, 9H). ¹³C NMR (125 Hz, DMSO-*d*₆) δ/ppm = 172.46, 172.14, 171.65, 171.30, 155.52, 137.90, 136.54, 130.18, 129.74, 128.45, 127.53, 126.68, 124.21, 121.44, 118.90, 118.42, 111.91, 109.65, 78.77, 53.95, 53.65, 52.27, 51.77, 37.97, 37.70, 28.63, 27.50.

4.2.18. Boc–Ser–Phe–Trp–OCH₃ (**n**)

HCl·Phe–Trp–OCH₃ (600 mg; 1.5 mmol) and Boc–Ser–OH (410 mg; 2.0 mmol) were combined to derive the end-product as a colorless solid (406 mg; 49% yield). Mp: 177–178 °C. ESI-MS (*m/e*) 553 [M + H]⁺; ¹H NMR (500 Hz, DMSO-*d*₆) δ/ppm = 10.89 (s, 1H), 8.51 (d, *J* = 7.0 Hz, 1H), 7.90 (d, *J* = 8.5 Hz, 1H), 7.49 (d, *J* = 8.0 Hz, 1H), 7.35 (d, *J* = 8.0 Hz, 1H), 7.34–7.17 (m, 6H), 7.10 (t, *J* = 7.5 Hz, 1H), 7.02 (t, *J* = 7.5 Hz, 1H), 6.69 (d, *J* = 8.0 Hz, 1H), 4.93 (t, *J* = 5.5 Hz, 1H), 4.59 (m, 1H), 4.52 (m, 1H), 3.97 (m, 1H), 3.56 (s, 3H), 3.46 (t, *J* = 6.0 Hz, 2H), 3.16 (dd, *J* = 6.0 Hz, *J* = 14.5 Hz, 1H), 3.07 (dd, *J* = 8.0 Hz, *J* = 15.0 Hz, 1H), 3.02 (dd, *J* = 9.5 Hz, *J* = 14.0 Hz, 1H), 2.79 (dd, *J* = 9.0 Hz, *J* = 13.5 Hz, 1H), 1.38 (s, 9H). ¹³C NMR (125 Hz, DMSO-*d*₆) δ/ppm = 172.43, 171.37, 170.52, 155.60, 137.92, 136.56, 129.76, 128.41, 127.51, 126.68, 124.19, 121.45, 118.91, 118.41, 111.20, 109.59, 78.72, 62.37, 57.30, 53.87, 53.68, 52.26, 37.97, 28.63, 27.54.

4.2.19. Boc–Tyr–Phe–Trp–OCH₃ (**o**)

HCl·Phe–Trp–OCH₃ (804 mg; 2.0 mmol) and Boc–Tyr–OH (560 mg; 2.0 mmol) were combined to derive the end-product as a colorless solid (1004 mg; 80% yield). Mp: 105–107 °C. ESI-MS (*m/e*) 629 [M + H]⁺; ¹H NMR (500 Hz, DMSO-*d*₆) δ/ppm = 10.89 (s, 1H), 9.15 (s, 1H), 8.55 (d, *J* = 7.5 Hz, 1H), 7.91 (d, *J* = 8.4 Hz, 1H), 7.49 (d, *J* = 7.8 Hz, 1H), 7.34 (d, *J* = 8.1 Hz, 1H), 7.26–7.16 (m, 6H), 7.07 (t, *J* = 7.5 Hz, 1H), 7.05–6.93 (m, 3H), 6.80 (d, *J* = 8.7 Hz, 1H), 6.61 (d, *J* = 8.4 Hz, 2H), 4.63 (m, 1H), 4.54 (m, 1H), 4.02 (m, 1H), 3.55 (s, 3H), 3.21–2.98 (m, 4H), 2.85–2.68 (m, 2H), 1.29 (s, 9H). ¹³C NMR (125 Hz, DMSO-*d*₆) δ/ppm = 172.44, 171.96, 171.52, 156.13, 155.52, 137.90, 136.53, 130.47, 129.81, 128.58, 128.43, 127.53, 126.71, 124.21, 121.43, 118.90, 118.42, 115.22, 111.89, 109.54, 103.51, 78.54, 56.63, 53.77, 53.60, 52.27, 38.27, 37.17, 28.58, 27.53.

4.2.20. Boc–Arg(NO₂)–Phe–Trp–OCH₃ (**p**)

HCl·Phe–Trp–OCH₃ (600 mg; 1.5 mmol) and Boc–Arg(NO₂)–OH (480 mg; 1.5 mmol) were combined to derive the end-product as a colorless solid (779 mg; 78% yield). Mp: 150–151 °C. ESI-MS (*m/e*) 667 [M + H]⁺; ¹H NMR (500 Hz, DMSO-*d*₆) δ/ppm = 10.88 (s, 1H), 8.54 (d, *J* = 5.0 Hz, 1H), 8.47 (s, 1H), 7.80 (d, *J* = 10.0 Hz, 1H), 7.49 (d, *J* = 5.0 Hz, 1H), 7.35 (d, *J* = 5.0 Hz, 1H), 7.25–7.15 (m, 6H), 7.08 (t, *J* = 7.5 Hz, 1H), 7.00 (t, *J* = 7.5 Hz, 1H), 7.00 (t, *J* = 7.5 Hz, 1H), 6.91 (d, *J* = 10.0 Hz, 1H), 4.63 (m, 1H), 4.54 (m, 1H), 3.86 (m, 1H), 3.56 (s, 3H), 3.17 (dd, *J* = 10.0 Hz, *J* = 15.0 Hz, 1H), 3.11–3.07 (m, 4H), 3.00 (dd, *J* = 5.0 Hz, *J* = 15.0 Hz, 1H), 2.80 (dd, *J* = 10.0 Hz, *J* = 15.0 Hz, 1H), 2.09 (s, 2H), 1.49–1.47 (m, 2H), 1.37 (s, 9H), 1.19 (m, 2H). ¹³C NMR (125 Hz, DMSO-*d*₆) δ/ppm = 172.47, 171.98, 171.47, 159.79, 155.69,

137.83, 136.55, 129.78, 128.40, 127.53, 126.69, 124.18, 121.45, 118.91, 118.42, 111.91, 105.57, 78.72, 54.64, 53.62, 52.27, 40.77, 38.26, 31.16, 29.68, 28.63, 27.52.

4.2.21. Boc-Asp(OCH₃)-Phe-Trp-OCH₃ (**q**)

HCl-Phe-Trp-OCH₃ (804 mg; 2.0 mmol) and Boc-Asp(OCH₃)-OH (480 mg; 2.0 mmol) were combined to derive the end-product as a colorless solid (962 mg; 81% yield). Mp: 161–162 °C. ESI-MS (*m/e*) 595 [M + H]⁺; ¹H NMR (500 Hz, DMSO-*d*₆) δ/ppm = 10.89 (s, 1H), 8.51 (d, *J* = 7.5 Hz, 1H), 7.79 (d, *J* = 8.5 Hz, 1H), 7.49 (d, *J* = 8.0 Hz, 1H), 7.35 (d, *J* = 8.0 Hz, 1H), 7.27–7.17 (m, 6H), 7.11 (d, *J* = 8.0 Hz, 1H), 7.08 (t, *J* = 7.5 Hz, 1H), 7.00 (t, *J* = 7.5 Hz, 1H), 4.58–4.52 (m, 2H), 4.29 (m, 1H), 3.57 (s, 3H), 3.56 (s, 3H), 3.17 (dd, *J* = 6.5 Hz, *J* = 14.5 Hz, 1H), 3.09 (dd, *J* = 7.5 Hz, *J* = 14.5 Hz, 1H), 2.99 (dd, *J* = 4.5 Hz, *J* = 14.0 Hz, 1H), 2.82 (dd, *J* = 8.5 Hz, *J* = 13.5 Hz, 1H), 2.61 (dd, *J* = 5.0 Hz, *J* = 16.0 Hz, 1H), 2.45 (dd, *J* = 9.0 Hz, *J* = 16.0 Hz, 1H), 1.37 (s, 9H). ¹³C NMR (125 Hz, DMSO-*d*₆) δ/ppm = 172.44, 171.21, 170.86, 155.59, 137.77, 136.55, 129.76, 128.62, 128.43, 127.53, 126.72, 124.17, 121.44, 118.90, 118.42, 111.90, 109.58, 78.93, 53.92, 53.60, 52.27, 51.95, 51.49, 38.09, 36.52, 28.59, 27.55.

4.2.22. Boc-Glu(OCH₃)-Phe-Trp-OCH₃ (**r**)

HCl-Phe-Trp-OCH₃ (804 mg; 2.0 mmol) and Boc-Glu(OCH₃)-OH (600 mg; 2.2 mmol) were combined to derive the end-product as a colorless solid (608 mg; 50% yield). Mp: 156–157 °C. ESI-MS (*m/e*) 609 [M + H]⁺; ¹H NMR (500 Hz, DMSO-*d*₆) δ/ppm = 10.88 (s, 1H), 8.55 (d, *J* = 5.0 Hz, 1H), 7.85 (d, *J* = 5.0 Hz, 1H), 7.49 (d, *J* = 10.0 Hz, 1H), 7.35 (d, *J* = 10.0 Hz, 1H), 7.23–7.17 (m, 6H), 7.08 (t, *J* = 7.5 Hz, 1H), 7.00 (t, *J* = 7.5 Hz, 1H), 6.92 (d, *J* = 10.0 Hz, 1H), 4.62 (m, 1H), 4.54 (m, 1H), 3.89 (m, 1H), 3.57 (s, 3H), 3.56 (s, 3H), 3.17 (dd, *J* = 5.0 Hz, *J* = 15.0 Hz, 1H), 3.10 (dd, *J* = 10.0 Hz, *J* = 15.0 Hz, 1H), 3.00 (dd, *J* = 5.0 Hz, *J* = 15.0 Hz, 1H), 2.79 (dd, *J* = 10.0 Hz, *J* = 15.0 Hz, 1H), 2.19 (t, *J* = 5.0 Hz, 2H), 1.78–1.64 (m, 2H), 1.37 (s, 9H). ¹³C NMR (125 Hz, DMSO-*d*₆) δ/ppm = 173.26, 172.45, 171.52, 155.60, 137.88, 136.55, 129.75, 128.39, 127.54, 126.68, 124.16, 121.43, 118.89, 109.57, 78.74, 54.12, 53.64, 52.25, 51.74, 38.20, 30.26, 28.61, 27.78, 27.52.

4.2.23. Preparation of HCl·L-AA-Phe-Trp-OCH₃

Solutions of **a–r** (2.0 mmol) in 10 mL of hydrogen chloride/acetate (4 mol/L) were stirred at 0 °C until TLC analysis indicated complete disappearance of the starting species (**a–r**). Following evaporation, the residue was dissolved in ethyl acetate (3 × 10 mL) and evaporated under reduced pressure to yield crude HCl·L-AA-Phe-Trp-OCH₃.

4.2.24. Preparation of **3a–r**

HOBt (6.0 mmol) was added to 4.6 mmol of **2** in 30 mL of anhydrous THF at 0 °C. After stirring for 10 min, 6.0 mmol of DCC was added. A suspension of 5.0 mmol HCl·L-AA-Phe-Trp-OCH₃ in 3 mL anhydrous THF was adjusted with *N*-methyl morpholine to pH 8–9 and then stirred at room temperature for another 20 min. This mixture was then added to solution of **2**, and the reaction mixture stirred at 0 °C for 2 h and then continued stirring at room temperature for 16 h. Following evaporation, the residue was dissolved in 30 mL of ethyl acetate. The solution was washed extensively with 5% sodium bicarbonate, 5% citric acid, and saturated sodium chloride, and the organic phase separated and dried over anhydrous sodium sulfate. Following filtration and evaporation under reduced pressure, *N*-(*N*-Boc-3*S*-1,2,3,4-tetrahydro-β-carboline-3-carboxyl)-L-AA-Phe-Trp methyl esters (**3a–r**) were obtained, which were deprotected without further purification.

4.2.25. Preparation of **4a–r**

A mixture of 0.2 mmol of **3a–r**, 1 mL of phenyl methyl ether, 1 mL of dimethyl sulfide, and 4 mL of HF was stirred at 0 °C for 2 h, followed by evaporation. The residue was supplemented with 1 mL

of phenyl methyl ether, 1 mL of dimethyl sulfide and 8 mL of HF and stirred at 0 °C for 2 h. The reaction mixture was evaporated under vacuum and the residue triturated with ether. The residue was then directly purified on Sephadex G-10 and HPLC to provide the desired product **4a–r**.

4.2.26. *N*-(3*S*-1,2,3,4-Tetrahydro-β-carboline-3-carboxyl)-Leu-Phe-Trp (**4a**)

Following deprotection, 0.2 mmol of **3a** yielded 107.2 mg of compound **4a** (81% yield). FAB-MS (*m/e*): 663 [M + H].

4.2.27. *N*-(3*S*-1,2,3,4-Tetrahydro-β-carboline-3-carboxyl)-Gly-Phe-Trp (**4b**)

Following deprotection, 0.2 mmol of **3b** yielded 94.5 mg of compound **4b** (78% yield). FAB-MS (*m/e*): 607 [M + H].

4.2.28. *N*-(3*S*-1,2,3,4-Tetrahydro-β-carboline-3-carboxyl)-Pro-Phe-Trp (**4c**)

Following deprotection, 0.2 mmol of **3c** yielded 95.6 mg of compound **4c** (74% yield). FAB-MS (*m/e*): 647 [M + H].

4.2.29. *N*-(3*S*-1,2,3,4-Tetrahydro-β-carboline-3-carboxyl)-Val-Phe-Trp (**4d**)

Following deprotection, 0.2 mmol of **3d** yielded 90.7 mg of compound **4d** (70% yield). FAB-MS (*m/e*): 649 [M + H].

4.2.30. *N*-(3*S*-1,2,3,4-Tetrahydro-β-carboline-3-carboxyl)-Ala-Phe-Trp (**4e**)

Following deprotection, 0.3 mmol of **3e** yielded 163.7 mg of compound **4e** (88% yield). FAB-MS (*m/e*): 621 [M + H].

4.2.31. *N*-(3*S*-1,2,3,4-Tetrahydro-β-carboline-3-carboxyl)-Phe-Phe-Trp (**4f**)

Following deprotection, 0.3 mmol of **3f** yielded 171.2 mg of compound **4f** (82% yield). FAB-MS (*m/e*): 697 [M + H].

4.2.32. *N*-(3*S*-1,2,3,4-Tetrahydro-β-carboline-3-carboxyl)-Ile-Phe-Trp (**4g**)

Following deprotection, 0.2 mmol of **3g** yielded 105.9 mg of compound **4g** (80% yield). FAB-MS (*m/e*): 663 [M + H].

4.2.33. *N*-(3*S*-1,2,3,4-Tetrahydro-β-carboline-3-carboxyl)-Trp-Phe-Trp (**4h**)

Following deprotection, 0.2 mmol of **3h** yielded 113.2 mg of compound **4h** (77% yield). FAB-MS (*m/e*): 736 [M + H].

4.2.34. *N*-(3*S*-1,2,3,4-Tetrahydro-β-carboline-3-carboxyl)-Thr-Phe-Trp (**4i**)

Following deprotection, 0.2 mmol of **3i** yielded 94.9 mg of compound **4i** (73% yield). FAB-MS (*m/e*): 651 [M + H].

4.2.35. *N*-(3*S*-1,2,3,4-Tetrahydro-β-carboline-3-carboxyl)-His-Phe-Trp (**4j**)

Following deprotection, 0.2 mmol of **3j** yielded 96.0 mg of compound **4j** (70% yield). FAB-MS (*m/e*): 687 [M + H].

4.2.36. *N*-(3*S*-1,2,3,4-Tetrahydro-β-carboline-3-carboxyl)-Lys-Phe-Trp (**4k**)

Following deprotection, 0.3 mmol of **3k** yielded 180.8 mg of compound **4k** (89% yield). FAB-MS (*m/e*): 678 [M + H].

4.2.37. *N*-(3*S*-1,2,3,4-Tetrahydro-β-carboline-3-carboxyl)-Gln-Phe-Trp (**4l**)

Following deprotection, 0.2 mmol of **3l** yielded 86.6 mg of compound **4l** (64% yield). FAB-MS (*m/e*): 678 [M + H].

4.2.38. *N*-(3*S*-1,2,3,4-Tetrahydro- β -carboline-3-carboxyl)-Asn-Phe-Trp (**4m**)

Following deprotection, 0.3 mmol of **3m** yielded 165.1 mg of compound **4m** (83% yield). FAB-MS (*m/e*): 664 [M + H].

4.2.39. *N*-(3*S*-1,2,3,4-Tetrahydro- β -carboline-3-carboxyl)-Ser-Phe-Trp (**4n**)

Following deprotection, 0.3 mmol of **3n** yielded 110.7 mg of compound **4n** (58% yield). FAB-MS (*m/e*): 637 [M + H].

4.2.40. *N*-(3*S*-1,2,3,4-Tetrahydro- β -carboline-3-carboxyl)-Tyr-Phe-Trp (**4o**)

Following deprotection, 0.3 mmol of **3o** yielded 164.5 mg of compound **4o** (77% yield). FAB-MS (*m/e*): 713 [M + H].

4.2.41. *N*-(3*S*-1,2,3,4-Tetrahydro- β -carboline-3-carboxyl)-Arg-Phe-Trp (**4p**)

Following deprotection, 0.3 mmol of **3p** yielded 158.6 mg of compound **4p** (75% yield). FAB-MS (*m/e*): 706 [M + H].

4.2.42. *N*-(3*S*-1,2,3,4-Tetrahydro- β -carboline-3-carboxyl)-Asp-Phe-Trp (**4q**)

Following deprotection, 0.3 mmol of **3q** yielded 157.4 mg of compound **4q** (79% yield). FAB-MS (*m/e*): 665 [M + H].

4.2.43. *N*-(3*S*-1,2,3,4-Tetrahydro- β -carboline-3-carboxyl)-Glu-Phe-Trp (**4r**)

Following deprotection, 0.3 mmol of **3r** yielded 111.8 mg of compound **4r** (55% yield). FAB-MS (*m/e*): 679 [M + H].

4.2.44. *H*-Leu-Phe-Trp-OH

Mp: 189–192 °C. ESI-MS (*m/e*) 465 [M + H]⁺; ¹H NMR (500 Hz, DMSO-*d*₆) δ /ppm = 12.36 (s, 1H), 10.98 (s, 1H), 8.82 (d, *J* = 8.0 Hz, 1H), 8.69 (d, *J* = 7.5 Hz, 1H), 8.22 (s, 2H), 7.50 (d, *J* = 7.5 Hz, 1H), 7.35 (d, *J* = 8.0 Hz, 1H), 7.29–7.23 (m, 5H), 7.21 (s, 1H), 7.08 (t, *J* = 7.5 Hz, 1H), 7.03 (t, *J* = 7.5 Hz, 1H), 4.64 (m, 1H), 4.49 (m, 1H), 3.73 (m, 1H), 3.18 (dd, *J* = 8.5 Hz, *J* = 15.0 Hz, 1H), 3.09 (dd, *J* = 7.5 Hz, 1H), 3.04 (dd, *J* = 4.5 Hz, *J* = 14.0 Hz, 1H), 2.86 (dd, *J* = 9.0 Hz, *J* = 14.0 Hz, 1H), 1.64 (m, 1H), 1.55–1.52 (m, 2H), 0.86 (t, *J* = 5.0 Hz, 6H). ¹³C NMR (125 Hz, DMSO-*d*₆) δ /ppm = 171.98, 171.21, 169.40, 137.98, 136.56, 129.68, 128.56, 127.54, 126.8, 124.31, 121.39, 118.83, 118.41, 111.89, 109.67.

4.2.45. *H*-Lys-Phe-Trp-OH

Mp: 268–269 °C. ESI-MS (*m/e*) 480 [M + H]⁺; ¹H NMR (500 Hz, DMSO-*d*₆) δ /ppm = 12.63 (s, 1H), 11.03 (s, 1H), 8.90 (d, *J* = 8.1 Hz, 1H), 8.55 (d, *J* = 7.5 Hz, 1H), 8.30 (s, 2H), 8.13 (s, 2H), 7.55 (d, *J* = 7.5 Hz, 1H), 7.36 (d, *J* = 8.1 Hz, 1H), 7.29–7.15 (m, 6H), 7.07 (t, *J* = 7.5 Hz, 1H), 6.99 (t, *J* = 7.5 Hz, 1H), 4.58 (m, 1H), 4.48 (m, 1H), 3.73 (m, 1H), 3.20 (dd, *J* = 5.1 Hz, *J* = 15.0 Hz, 1H), 3.09 (dd, *J* = 8.4 Hz, *J* = 15.0 Hz, 1H), 3.01 (m, 1H), 2.85 (dd, *J* = 9.9 Hz, *J* = 13.5 Hz, 1H), 2.72 (m, 2H), 1.76 (m, 2H), 1.55 (m, 2H), 1.36 (m, 2H). ¹³C NMR (125 Hz, DMSO-*d*₆) δ /ppm = 173.59, 171.31, 168.97, 138.06, 136.53, 129.73, 128.54, 127.63, 126.79, 124.36, 121.32, 118.93, 118.57, 111.88, 110.03, 54.99, 53.53, 52.25, 38.58, 37.75, 30.67, 27.48, 26.56, 21.30.

4.3. Biological assays

All animal experiments were performed in compliance with the "Guide for the Care and Use of Laboratory Animals" published by the US National Institutes of Health.

4.3.1. Analysis of *in vivo* pain threshold

Male ICR mice (20 ± 2 g) were housed in a 12/12 light/dark cycle at 21 ± 2 °C for 24 h before use. Pain threshold for each mouse was measured in triplicate. Analgesic effects of synthetic compounds

were evaluated by the tail flick test. Subjects received a single gavage of each synthetic compound (0.15 mmol/kg in 0.2 mL of saline mixed with 0.3% CMC-Na). The control cohort received vehicle only. Pain thresholds were measured 30 min after oral administration at 30 min intervals for a total of 3 h. Evaluations were terminated if the animal did not respond within 10 s in order to avoid tissue damage. The potency of analgesia was estimated by the pain threshold variation (PTV). The values were calculated as PTV = AAPT ÷ BPT where BPT = basic pain threshold and AAPT = pain threshold after administration – basic pain threshold. All values over 3 h were averaged and constituted one determination (repeated in triplicate). Statistical analysis employed one-way ANOVA with *P* < 0.05 as the measure of significance.

4.3.2. Evaluation of *in vivo* anti-inflammatory activity

Anti-inflammatory activities of new compounds were evaluated in a xylene-induced ear edema assay. Briefly, male ICR mice (20 ± 2 g) were randomly divided into three groups, including the test group, vehicle control (1% Carboxymethyl cellulose solution, CMC) and positive control group (aspirin). The positive control cohort received an oral suspension of aspirin in CMC (10 mg/kg). The test group received oral suspensions of test species in CMC (0.15 mmol/kg) initially. Thirty minutes later, 0.03 mL of xylene was applied to the anterior and posterior surfaces of the right ear, the left ear serving as control. Two hours following xylene application, the mice were sacrificed and both ears were removed. Multiple circular sections were obtained using a cork borer (diameter 7 mm) and weighed. The increase in weight reflected by xylene irritation was determined by subtracting the weight of untreated tissue sections from treated sections.

4.3.3. Intestinal ischemia/reperfusion model

Male Wistar rats (250–300 g) were randomly allocated into 3 groups: (1) sham group: rats subjected to the procedures described below, with the exception of ischemia/reperfusion (I/R) (*n* = 6); (2) I/R group: rats subjected to the procedures described below undergoing intestinal ischemia for 45 min followed by reperfusion for 3 h (*n* = 8); (3) I/R + drug treatment group: rats received melatonin or **4a** (20 mg/kg) 15 min prior to reperfusion and again 1 h following initiation of reperfusion (*n* = 8). Animals in groups (1) and (2) were administered saline vehicle in lieu of drug. Male Wistar rats were anesthetized with an intraperitoneal injection of sodium pentobarbital (80 mg/kg). Throughout the experiment body temperature was maintained at 37 °C with the aid of a heating pad. Laparotomy was performed through a midline incision into the peritoneal cavity. The small bowel was gently exposed on moist gauze, followed by occlusion of the superior mesenteric artery for 45 min using a microvascular clamp, with 3 h reperfusion afterward. Surgical incisions were closed during the reperfusion period. Sham-operated rats underwent an identical surgical protocol but did not undergo superior mesenteric artery clamping and were anesthetized for the duration of the experiment. Fifteen minutes prior to reperfusion, and 1 h after initiation of reperfusion, melatonin or **4a** (20 mg/kg) was administered intraperitoneally to rats assigned to I/R + drug treatment group, while sham subjects received only saline. Subjects were sacrificed by sodium pentobarbital overdose at the conclusion of all studies and small intestine tissues were immediately harvested in addition to blood sampling from the ascending aorta. Tissue samples were divided into two parts, one for determination of lipid peroxidation, and other for microtome sectioning (Leica CM1850 UV clinical cryostat) at –30 °C.

4.3.4. Malondialdehyde (MDA) and glutathione (GSH) assays

MDA represents a stable product of oxidative degradation of polyunsaturated fatty acids, and indicates the level of cellular

damage secondary to lipid peroxidation. Accordingly, MDA levels are routinely employed as a measure of free radical formation under oxidative stress conditions. MDA levels were determined following the method of Beuge and Aust [17], and expressed as nmol/g tissue. GSH was determined using Beutler's method and expressed as $\mu\text{mol/g}$ tissue [18].

4.3.5. Evaluation of myeloperoxidase (MPO) activity

Tissue-associated MPO activity was measured as described [20] and expressed in U/g tissue.

Statistical analysis: A two-way ANOVA followed by Scheffé's test was initially performed using the Origin Program to test for differences between groups. If differences were observed, the values were compared using Student's *t*-test for paired data. The values were expressed as means \pm SD, and considered significant if $P < 0.05$.

4.3.6. Histological analysis

Strips of terminal ileum at 10 mm length were immediately removed upon completion of the ischemia/reperfusion procedure and euthanization. The specimen was mounted in gum tragacanth in the correct orientation and snap-frozen in isopentane chilled in liquid nitrogen. The frozen tissue sections (4–5 μm) were then cut using a cryostat microtome (Leica CM1850 UV clinical cryostat) at -30°C , stained with hematoxylin–eosin, and examined under light phase (Olympus-BX51).

4.4. Molecular dynamic simulation

Molecular dynamic evaluations were performed based on the MM2 force field (CambridgeSoft Chem & Bio 3D 12.0). Parameters employed included: step interval: 2.0 fs; frame interval: 10 fs; terminate after: 10,000 steps; heating/cooling rate: 1.000 kcal/atom/ps; target temperature: 300 K.

Acknowledgments

The authors are grateful to NASA (MSGC R85197), Research Excellence Fund (R01121), Natural Science Foundation of HeBei,

China (No. 062761266) and the Administration of Traditional Chinese Medicine of HeBei Province (No. 2007134), for support of this research. The authors are also grateful to Professor Herve Galons for many helpful suggestions.

References

- [1] G.S. Herbert, S.R. Steele, *Surg. Clin. North Am.* 87 (2007) 1115.
- [2] A. Khanna, J.E. Rossman, H.L. Fung, *J. Surg. Res.* 99 (2001) 114.
- [3] P.A. Ward, G.O. Till, J.S. Warren, *J. Crit. Care* 6 (1991) 112.
- [4] G.J. García-Rivas, G. Torre-Amione, *Methodist DeBakey Cardiovasc. J.* 5 (2009) 2–7.
- [5] A.D. Rodríguez, P.A. González, *Rev. Esp. Cardiol.* 62 (2009) 952–953.
- [6] T. Berland, W.A. Oldenburg, *Curr. Gastroenterol. Rep.* 10 (2008) 341–346.
- [7] M. Sasaki, T. Joh, *J. Clin. Biochem. Nutr.* 40 (2007) 1–12.
- [8] M. Ham, J.D. Kaunitz, *Curr. Opin. Gastroenterol.* 24 (2008) 665–673.
- [9] S.Y.H. Tse, I.T. Mak, B.F. Dickens, *Biochem. Pharmacol.* 42 (1991) 459–464.
- [10] H.H. Kim, Y.Y. Jang, E.S. Han, C.S. Lee, *J. Appl. Pharmacol.* 7 (1999) 112–120.
- [11] C.S. Lee, E.S. Han, Y.Y. Jang, J.H. Han, H.W. Ha, D.E. Kim, *J. Neurochem.* 75 (2000) 521–531.
- [12] D.H. Kim, Y.Y. Jang, E.S. Han, C.S. Lee, *Eur. J. Neurosci.* 13 (2001) 1861–1872.
- [13] T.H. Park, O.S. Kwon, S.Y. Park, E.S. Han, C.S. Lee, *Neurosci. Res.* 46 (2003) 349–358.
- [14] A. Shulov, S. Shulov, N. Primor, *US Pat No* 7,220,725 B2.
- [15] F.J. Vocci, S.K. Petty, W.L. Dewey, *J. Pharmacol. Exp. Ther.* 207 (1978) 892–894.
- [16] M. Medakovic, B. Banic, *J. Pharm. Pharmacol.* 16 (1964) 198–206.
- [17] (a) L. Bi, Y. Zhang, M. Zhao, C. Wang, J. Tok, S. Peng, *Bioorg. Med. Chem.* 13 (2005) 5640–5646;
(b) K. Gu, L. Bi, M. Zhao, C. Wang, J. Ju, S. Peng, *Bioorg. Med. Chem.* 15 (2007) 4775–4799;
(c) K. Gu, L. Bi, M. Zhao, C. Wang, J. Ju, S. Peng, *Bioorg. Med. Chem.* (2007) 6273–6290;
(d) K. Gu, L. Bi, M. Zhao, C. Wang, J. Tok, S. Peng, *Bioorg. Med. Chem.* 14 (2006) 1339–1347;
(e) L. Bi, M. Zhao, K. Gu, C. Wang, J. Ju, S. Peng, *Bioorg. Med. Chem.* 16 (2008) 1764–1774.
- [18] J.A. Buege, S.D. Aust, *Methods Enzymol.* 52 (1978) 302.
- [19] E. Beutler, *A Manual of Biochemical Methods*. Grune and Stratton, New York, 1975, pp. 112–114.
- [20] D.P. Jones, *Antioxid. Redox Signal.* 8 (2006) 1865–1879.
- [21] L.M. Hillegass, D.E. Griswold, B. Brickson, C. Albrightson-Winslow, *J. Pharmacol. Methods* 24 (1990) 285–295.
- [22] I.H. Mallick, W. Yang, M.C. Winslet, A.M. Seifaian, *Dig. Dis. Sci.* 49 (2004) 1359–1377.
- [23] C.D. Collard, S. Gelman, *Anesthesiology* 94 (2001) 1133–1138.
- [24] A. Mohajeri, S.S. Asemani, *J. Mol. Struct.* 930 (2009) 15–20.
- [25] F.C. Lavarda, *Int. J. Quant. Chem.* 95 (2003) 219–223.